STATUS OF THE LMFBR THERMO- AND FLUID-DYNAMIC ACTIVITIES AT KFK

H. HOFFMANN, F. HOFMANN, K. REHME
Kernforschungszentrum Karlsruhe,
Karlsruhe,
Federal Republic of Germany

1. Introduction

The aim of the thermo- and fluiddynamic analysis is to determine the spatial velocity and temperature distributions in LMFBR-core elements with high accuracy. Knowledge of these data is a necessary prerequisite for determining the mechanical behavior of fuel rods and of structural material.
Three cases are distinguished:

- Nominal geometry and steady state conditions
- Non-nominal geometry and quasi-steady state conditions
- Nominal geometry and non-steady state conditions.

The present situation for the design calculations of fuel elements is based mainly on undisturbed normal operation.

The most part of the thermo- and fluiddynamic activities performed under the Fast Breeder Programme at KFK are related to this case.

The present status of theoretical and experimental research work briefly presented in this paper, can be subdivided into the following main topics:

I. Physical and mathematical modelling of single phase rod bundle thermo- and fluiddynamics

These investigations are concentrated on the development of global and local computer programs for the calculation of the 3-dim. temperature field of the fuel pin, the fuel rod bundle, and the whole core. Heat conduction between the subassembly boxes as well as asymmetric bundle geomtries are considered. Further code developments deal with the hot spot analysis.

II. Experimental Investigations on Heat Transfer and Fluid Flow in Rod Bundles

These investigations aim at the verification and improvement of the input parameters of the global and local computer codes. The experimental activities concern:

a) Pressure drops of laminar and turbulent flows in rod bundles without and with spacers, helical and grid spacers, and their dependence on geometry parameters and the Reynolds number
b) Interchannel mixing in rod bundles with grids or helical spacers
c) Temperature distributions in rod bundles without and with spacers, with particular reference to cladding temperatures,
d) Velocity and mass flow distributions in rod bundles without and with grid spacers.

Non-nominal geometry and quasi-steady state conditions include local disturbances of the flow within the subassembly (e.g. swelling, bowing, effects which are a function of operation time).

In the next step of our R and D-program emphasis will be put on this topic. Up to now experiments with bowed rods have been performed. Problems with respect to non-steady thermo- and fluiddynamics will be dealt with mainly within the framework of accident analyses and will not be considered in this paper.

2. Physical and Mathematical Modelling of Single Phase Rod Bundle Thermo- and Fluiddynamics

The codes presently available for the computation of fuel elements can be subdivided into two categories:

- global codes for subchannel analysis
- detailed codes for multidimensional calculation of the velocity and temperature fields.

Both categories comprise only the single-phase region (Fig. 1).

2.1 Global Codes

Thermo- and fluiddynamic design calculations are performed by the so called subchannel analysis technique, i.e. the mass flow distribution in the subchannels is calculated only globally (mean value). As a consequence, it is impossible to calculate with sufficient

accuracy the behavior of fuel rods with respect to detailed temperature distribution in the cladding, especially near the wrapper tube. The reason for the procedure adopted so far, on the one hand, is the absence of computer programs for detailed analysis, on the other hand, the lack of experimental information about flow and temperature distributions in subchannels of subassemblies which could either be used as input data for such computer programs or are necessary to back up the codes.

In the global codes typically the subassembly geometry to be calculated is subdivided into a matrix of subchannels. Such a subchannel comprises the fuel rod, the fluid region, the spacers and the wrapper tube. For each of the subchannels the balance equations of mass, momentum and energy are set up and solved numerically for the desired matrix (determination of mean values). Coupling at the boundaries of the different subchannels by the transports of mass, momentum and energy is done by way of global coefficients, in the simplest case by a mixing coefficient describing the three transport phenomena, in the more refined case by special treatment of thermal conduction, turbulent mixing and diversion cross flow. The main advantage of the techniques lies in the coupling and calculation even of complicated geometries of the fuel element, taking into account both grid and helical spacer designs. The calculations can now also be carried out for three-dimensional flows under steady-state conditions, whereas mixed convection events such as those which may occur in greatly throttled flows are not taken into account (part load).

For fuel element design the following codes are available at KFK:

MISTRAL II	/1/
ARTIS	/2/
THECA	/3/

MISTRAL II-Code

The code permits the steady-state three-dimensional calculation of the bulk temperatures and velocities in a rod subassembly (7 to 217 rods) with triangular rod arrangements and spacers (grids and wires). The momentum and energy equations are solved by the finite difference method. The grid drag is considered to be smeared over the length of the subassembly. The pressure loss is calculated by

$$\Delta p = -\left(\frac{\dot{m}}{F}\right)^2 \frac{L}{2g}\left(\frac{\lambda}{D_h} + \frac{if}{L}\right) \qquad (1)$$

For the central zones of the subassembly and the exchange between the inner channels and the side channels a global mixing rate is used which is obtained experimentally for a hexagonal array of infinite extensions /4/:

$$q_{ij} = \mu \cdot \dot{m} \cdot \Delta h \qquad (2)$$

In the case of grid type spacers this mixing ratio is corrected for the exchange among side channels by the ratio of the free distances between rods and between rods and the wall, respectively.

In the case of helical spacers the additional exchange coefficient of the boundary channels in the code is calculated according to

$$\mu_R = \frac{D \cdot \pi \cdot S \cdot EF}{F_K \cdot H} \qquad (3)$$

Thermal conduction in the coolant is represented in the program by a thermal conduction pathway which has the mean channel temperatures at both ends;

$$q_{iz} = k \cdot \Delta T \frac{\Delta s}{\Delta y} \qquad (4)$$

Thermal conduction in the rod or wrapper tube is neglected.

The code allows the consideration of rod bundles excentrically positioned inside the wrapper tube.

ARTIS Code

In the ARTIS computer program for hexagonal rod arrangements in different axial steps the balance equations for mass and enthalpy are solved for each subchannel with its cross connections to the neighboring channels. In the solution of the coupled system of equations, unlike MISTRAL II, the following effects are taken into account separately: wall friction, impact losses, radial and azimuthal turbulent momentum and energy transports (coolant cross mixing), mass redistribution due to friction and drag.

The exchange of momentum and energy is described in the following physical model setups:

Momentum Transport:

$$I = - \varepsilon_{M_r} \cdot s \cdot \frac{\Delta u}{\Delta y} \frac{\varepsilon_{M\varphi}}{\varepsilon_{M_r}} \qquad (5)$$

Energy Transport:

$$q = - \psi \cdot \varepsilon_{M_r} \cdot s \frac{\Delta u}{\Delta y} \qquad (6)$$

All these equations are related to each individual subchannel.

Due to the model of net mass transport it is only possible to take into account grid type spacers in the ARTIS program. The size of the subassembly does not raise any problems. Beside the whole subassembly any section of the subassembly can be calculated. For each channel an individual mass flow and power can be considered as input (e.g., for simulation of non-uniform mass flow distribution at the inlet or γ-heating of the wrapper tube.

The program also allows individual rods to be assumed as displaced or bent and their effects on mass and temperature distributions to be calculated.

THECA Code

While the MISTRAL and ARTIS code mainly serve for the design of single fuel elements, the THECA code is concentrated chiefly on determining the temperature distribution throughout the core (with shutdown positions, with various enrichment zones), taking into account heat transfer between the fuel elements. At the same time, this is connected with a detailed hot spot analysis.

The temperature distribution in the individual elements is determined in a way similar to the procedure adopted in the MISTRAL code.

Up to four types of rod subassemblies can be computed (e.g., fuel elements, blanket elements, control rods, shutdown rods).

The necessary power distribution can be computed in two ways:

(1) by inputting the axial development of the linear rod powers at 7 support points per subassembly: central rod and 6 corner rods and proper interpolation;

(2) by transferring the neutron flux distribution and fission cross sections from a neutron physics diffusion program.

For calculation of the temperature distribution throughout the whole core or a representative core section the power data can be quoted individually for each position (consideration of local flux and power depressions, respectively). For calculation of the γ-heating in the wrapper tube the input of axial gamma heating rates depending on position and time is possible.

The thermal interaction between the different subassemblies is treated as a thermal conductivity problem. The real geometry is replaced by a network connecting the center points of the individual computation meshes by so-called "thermal conductivity pathways". (Fig. 2). Each thermal conductivity pathway is assigned the heat transport coefficient resulting for the volume element represented by the thermal conductivity pathway. In this way, an energy balance can be drafted for each center of a mesh.
In the wrapper tube/coolant channel coupling the pertinent heat transfer coefficient α_{KM} is not easily determined. The situation roughly resembles a flat plate type flow in which one side (fuel rods) is heated strongly, whereas the other is heated only weakly or even cooled, depending on whether heat flows through the box wall into or out of the subassembly.

In a simplified assumption for the heat transfer between the box wall and the coolant channel the heat transfer coefficient of an inner channel is assumed as a reference value. By adding the suitable input parameters this value can be corrected in accordance with the direction of the heat flow.

If there should be a leakage flow in the gap between the box walls a one-dimensional flow design is assumed. In a simplified technique the heat transfer coefficient of a laminar, fully developed and symmetrically heated flat plate flow is assumed.

Besides determining the nominal temperature distributions, THECA determines the quantitative connections between the occurrence of overtemperatures and overpowers, respectively, and the pertinent probability values. The uncertainties entering the analysis are broken down into groups in accordance with their different effects: into local, channel, fuel element, zone and core uncertainties. A local uncertainty will influence each point of the core in a statistically independent way, whereas a core uncertainty acts uniformly on all parts of the core.

On the basis of the nominal temperature distribution the probability of critical temperature or power levels being exceeded is calculated for each computation mesh and integrated to probability values applying to the whole core, taking into account the different effects of the individual uncertainties.

2.2 Detailed Codes

The methods used for the global codes are only able to indicate mean channel temperatures and have difficulties in applying in the boundary and edge areas of hexagonal fuel element boxes, as well as for distorted geometries, which are zones of special relevance. Local fluid and fuel rod surface temperatures cannot be calculated directly. The fuel rod surface temperature is calculated by an empirical Nusselt relation, a method which leads to major inaccuracies especially in the boundary and edge zones.

For this reason, detailed codes are required to describe local effects.

The codes belonging in this category are based on the multi-dimensional solution of the steady-state Navier-Stokes and energy equations to determine local velocity and temperature distributions. Geometrically they are restricted to the assessment of individual subchannels or a small number of subchannels of one fuel subassembly. The main drawback at present is the inability to take into account spacers (grids and helices). The main objectives of these codes are

- a more accurate assessment of the temperature distribution in the cladding of the individual fuel rods, especially in the boundary zones of the fuel elements
- backup of the global codes by
  - improved description of physical processes
  - derivation of improved global coefficients (mixing, heat transfer) as input to the subchannel codes.

The following codes are available:

VELASCO-Code /5/

This code developed by Eifler and Nijsing (Ispra) calculates the detailed velocity and wall shear stress distributions in subchannels of rod subassemblies.

The physical model involves the assumption, that a flow section can be divided into "momentum-balanced" zones around the wetted walls, bounded in the liquid by "zero-shear"-lines, i.e. lines perpendicular to which the momentum flux is zero. These zones, in principle closed around a wetted wall, may be divided in two or more identical parts by radial symmetry lines. The radial extent of the momentum-balanced zones is a priori only known for the particular case where the zero shear line coincides with a symmetry line.

Fig. 3 shows as an example the case of a thirty-seven rod array in a hexagonal channel.

Within one zone a momentum balance for a differential volume element $r\,d\varphi\,dr\,dz$ yields under conditions of steady flow

$$\frac{\partial(\bar{\tau}_r r)}{\partial r} + \frac{\partial(\bar{\tau}_\varphi)}{\partial \varphi} = -\frac{\partial p}{\partial z} r \qquad (7)$$

r, φ and z are the radial, peripheral and axial coordinate respectively, $\bar{\tau}_r$ and $\bar{\tau}_\varphi$ represent the momentum fluxes in the r and φ direction respectively. With the assumption of fully developed flow, the pressure gradient $\partial p/\partial z$ becomes constant and can be

determined from a momentum balance applied to the entire flow section:

$$-\frac{\partial p}{\partial z} = \frac{4\,\bar{\tau}_{w,av}}{d_h} \qquad (8)$$

$\bar{\tau}_{w,av}$ is the average wall shear stress, d_h the hydraulic diameter of the rod array considered.

For the determination of the radial velocity distribution different expressions are used for:

wall region:

$$u^+ = y^+\left(1 - 0.34\frac{y^+}{u_o^+} + 0.039\left(\frac{y^+}{u_o^+}\right)^2\right) \qquad (9)$$

For the center region of smooth channels the following expression was derived:

$$u^+ = \frac{1}{\kappa}\ln y^+ + C + \frac{1}{\kappa}\ln\frac{T_e(2-Y)}{2\left[1+(T_e-1)(1+Y)^2\right]} \qquad (10)$$

The parameters u^+ and y^+ are defined as

$$u^+ = \frac{u}{\sqrt{\frac{\bar{\tau}_w}{\rho}}} \qquad y^+ = \frac{(r-R)\sqrt{\frac{\bar{\tau}_w}{\rho}}}{\nu} \qquad (11)$$

U_o^+ is a constant and has the value 14.7 . y_o^+ is a measure for the thickness of the viscous wall region, which is assumed to have the value 21 . κ and Te are parameters depending primarily on the local geometry.

The momentum flux $\bar{\tau}_\varphi$ is assumed to be made up of a turbulent diffusion and of a convective transport term, as expressed by

$$\bar{\tau}_\varphi = \rho\,\varepsilon_{M\varphi}\cdot\frac{\partial u}{r\,\partial\varphi} + \rho\,u\,v \qquad (12)$$

τ_φ is the eddy diffusivity for momentum transport in the peripheral direction, ρ is the density of the fluid, U is the axial velocity and v the peripheral secondary flow component.

$\varepsilon_{M\varphi}$ was found to be represented well by the relation

$$\varepsilon_{M\varphi} = 0.154\sqrt{\frac{\bar{\tau}_w}{\rho}}\,(r_m - R) \qquad (13)$$

For the peripheral secondary flow component v the previously given expression

$$v = 2\,C_{sec}\,\frac{s_{e\,sec}}{s_e}\cdot\frac{d\sqrt{\frac{\bar{\tau}_w}{\rho}}}{dX}\cos(\pi Y) \qquad (14)$$

is used with

$$C_{sec} = 0.573 \qquad (15)$$

$s_{e_{sec}}$ is the peripheral extent along the wall of a closed secondary flow vortex.

Because of major deviations from existing experimental results especially for low P/D-ratios the model setups for anisotropy and secondary flow are in need of revision.

VERA-TERA-Code

The program system calculates the velocity and temperature fields of turbulent flows in subchannels of rod assemblies by means of curvilinear-orthogonal coordinates (Fig. 4).

VERA/TERA mainly consists of two modules, namely the module needed to establish the system of coordinates and the module used to calculate the flow; both modules are available in two variations, for central and for wall channels.

In calculating the velocity and temperature fields anisotropic transport of momentum and heat is taken into account.

The eddy viscosity normal to the wall, ε_{M_r}, is determined by Prandtl's mixing length theorem /7/, while the mixing length is calculated by means of Nikuradse's realtion /9/ corrected by Van Driest /8/:

$$\varepsilon_{M_r} = \left[\left\{1 - \exp(-y^+/26)\right\}^2 \hat{y}\left\{0.14 - 0.08\,(1-y/\hat{y})^2 - 0.06\,(1-y/\hat{y})^4\right\}\right]^2 \left|\frac{\partial \bar{u}_1}{\partial x_2}\right| \qquad (16)$$

The eddy viscosity parallel to the wall is also calculated by Prandtl's mixing length theorem:

$$\varepsilon_{M_\varphi} = \ell_2^2 \left|\frac{\partial \bar{u}_1}{\partial x_3}\right| \qquad (17)$$

where $\partial \bar{u}_1/\partial x_2$ means the maximum velocity grandient normal to the wall, $\partial \bar{u}_1/\partial x_3$ the maximum azimuthal velocity gradient. For calculation of the mixing length l_2 a ramp function according to /1/ is applied.

$$l_2 = \begin{cases} my & \ell_2 < 0.14\hat{y} \\ 0.14\,\hat{y} & \text{at other points} \end{cases} \qquad (18)$$

Wall channels are treated in an analogous manner.

The eddy conductivity ε_H can be determined from the eddy viscosity ε_M by means of a suitable conversion function $\Psi = \varepsilon_H/\varepsilon_M$. VERA/TERA can be used for this conversion to be made by means of different relations /1o/.

Presently one central channel and one wall channel versions are available. The model for the exchange of momentum needs to be improved, coupling of the subchannels is required.

This coupling is already included in the VITESSE code /11/ developed by Slagter (ECN). For this reason, this code is presently used for interpretation of KFK-experiments and is also being developed further.

TURBIT-3 Code /12,13/

The TURBIT code was developed for numerical simulation, by means of a finite difference method, of non-steady state, three dimensional turbulent flow and temperature fields in channel flows for fluids of constant physical properties. The method is based on a difference form of the complete equations of the conservation of mass, momentum including buoyancy terms, and enthalpy. The fluxes of momentum and heat within the grid cells are described by sub-grid scale models. The momentum sub-grid scale model introduced here is applicable to low Reynolds numbers, rather coarse grids and to channels with space dependent roughness distributions. The temperature sub-grid scale model introduced in addition takes into account the influence of the molecular Prandtl number. At the very low molecular Prandtl number of liquid metals the model shows that complete resolution of all relevant temperature-fluctuations can be achieved on the basis of presently realizable grids.

The method allows the simulation of laminar and turbulent flows in parallel plane channels and concentric annuli. In addition to pure forced convection, both forced convection influenced by bouyancy and also pure natural convection can be taken into account (Bernard convection and Rayleigh convection).

The numerical results for the flow field show a slight influence of changes in model parameters. Agreement with experimental results is fairly good for smooth, rough and partly roughed channels with secondary flows, even when rather coarse grids are used. The simulated temperature fields are very insensitive to changes of model parameters. The results determined numerically are in good agreement with consistent, reliable experimental results /12/. The accuracy of the numerical results makes it possible to compute quantities which so far have not been determined experimentally, but which are of decisive importance in the development of higher order statistical turbulence models.

2.3 Assessment of the Global Codes Used for Design Calculations

The existing subchannel codes are similar in structure. However, they use different models for momentum and energy exchange between

adjacent subchannels. To examine the qualitiy of such codes, intercomparison calculations were performed in two steps within the framework of Kerntechnische Gesellschaft/Fachgruppe Thermo- und Fluiddynamik.

Step_1 /14/:

The mean subchannel temperatures, the wall temperatures around the circumference of rods and wrapper tubes, and pressure losses were precalculated for subassemblies with the following distinguishing features:

- different rod numbers (19 and 61)
- different rod arrangements (P/D, W/D ratios)
- different types of spacers (grids, helical wires)
- different types of heating (numbers and positions of heated rods in the subassemblies).

The criteria for distinction and the operating conditions were taken from existing experimental results which, however, were not generally known and which should be used for comparison with the computed results. In some cases e.g., the problems implied extreme load cases not to be expected in a core element. The computer programs for this reason had to meet requirements which they would not have to meet normally.

The results of this intercomparison study can be described as follows and, at the same time, demonstrates the need for further code improvements and experiments:

- The precalculated pressure drops differ by up to 15%
- comparison of the precalculated temperatures shows that
  . trends are generally predicted correctly
  . peak temperatures are generally precalculated at the same levels
  . the variations of mean coolant temperatures and the respective wall temperatures on the circumference of characteristic rods differ greatly in some cases (by a factor of 2),
- Comparison between precalculated temperatures and those determined experimentally shows that the precalculated values agree with experimental findings only trendwise, and do so the better the simpler the subassembly geometries were and the less complicated the thermodynamic and fluid-dynamic conditions were.

For comparison the computed and experimental mean subchannel temperatures are shown in Fig. 5 for the example of a 61-rod subassembly with grid type spacers and only two heated rods (central rod/rod in the center of the row near the wall).

Step_2_/15/:

Supplementary to the thermodynamic calculations of step 1 calculations were performed for a fully heated 61 rod subassembly with the following conditions:

- with and without power gradient over the subassembly cross section
- cosine shaped axial power distribution
- grid and helical wire type spacers.

The following parameters had to be calculated:

- the mean mass flow rates of the subchannels,
- the mean coolant temperatures in the subchannels
  . at the end of the heated subassembly section (core end)
  . at the end of the upper blanket (end of subassembly)
- the pressure drops over the lengths of the subassemblies.

No experimental results were available for the studies. Accordingly, intercomparison of the results was possible only for the computed values.

Again the result can be summarized briefly and indicates the direction in which further studies must be performed:

- Precalculation of pressure drops leads to satisfactory results (deviations $< 7\%$)
- Comparison of precalculated temperatures shows that
  . trends are generally predicted correctly
  . the maximum levels of temperatures differ from each other by up to 15% of the temperature rise

. temperature variations around the circumferences of rods and the subchannels adjacent to the wrapper tube again show major differences
. the locations of the maximum temperatures within the cross section are precalculated for different subchannels by the individual codes.

- Comparison of calculated subchannel mass flows, which determines the temperature variations, shows that
  . precalculations agree well in the central area,
  . precalculations differ greatly in the wall area(by a factor of 2).

For comparison the mean subchannel coolant temperatures and the mean subchannel mass flows calculated for the core end are shown in Fig. 6 for the example of a 61-rod subassembly with grid type spacers and different power outputs per row of rods.

The following general comments can be made on these results: The results compared in this case were calculated by different participants by means of codes of different development statuses.

However, this changes nothing in the fact that also comparable codes precalculate greatly varying results.

3. Experimental Investigations on Heat Transfer and Fluid Flow in Rod Bundles

3.1 Global Studies

In order to obtain precise input data for the computer programs a number of experimental studies were conducted in the past. The loss of pressure in rod subassemblies without spacers was studied over a wide range of parameters (P/D, W/D, number of rods and arrangement). On the basis of the results an upper limit for the loss-of-pressure coefficient was indicated /16,17/. For the loss-of-pressure coefficient in the subchannels of rod subassemblies a method was developed to compute values for turbulent flows from the laminar solution /18, 19/.

A number of pressure drop studies were conducted on rod bundles with grid type spacers /2o-23/. In this connection it was also studied in what way the leading edge of the spacer grid influences the grid drag. Fig. 7 shows drag coefficients of grids in a rod subassembly consisting of 12 rods.

In order to influence the drag coefficient of the original grid design (SI) the leading edge was chamfered. Because of burr caused by the working process this resulted in an increase in the drag coefficient (SII). As a consequence, the blockage of the flow cross section by the grid of ε = o.348 (SI and SII) was reduced to ε = o.28 (SIII). Despite a sharp leading edge the drag coefficient was reduced considerably (SIIIS). Rounding of the leading edge (SIIIR) greatly reduced the drag coefficient even further /23/.

Pressure drop investigations on rod subassemblies with helical wire spacers were carried out over a wide range of parameters (P/D; H/D; number of rods) /24/. All results were covered byone computation model. For this purpose, a modified velocity was introduced which takes into account the geometric data of the subassemblies. The applicability of the model was extended also to subassemblies with helical fin tubes /4/. Additional pressure drop measurements using subassemblies with helical spacers and very low P/D-ratios ($1.0 \leq P/D \leq 1.15$) were carried out/25/. The results for $Re = 10^5$ of all these experiments are shown in Fig. 8, where the friction factors referring to the smooth tube are plotted versus P/D, the helical lead to rod diameter ratio H/D being the parameter of interest.

The magnitude of coolant cross mixing (mixing ratio) was determined in subassemblies with grid type and helical spacers /4; 26; 27; 28/. These results were obtained especially for those subchannel programs which consider the influences of spacers on thermodynamics and fluid dynamics as values averaged over the length of a subassembly. For this reason, the results embody all transport parameters globally (mass, momentum, energy), because a separation into individual quantities was not possible. In the studies pertaining to grid type spacers /27/ the geometry of

the grid and the number of grids in the subassembly was varied, in the studies with helical spacers /4, 26, 28/ the type of spacer(wire, fins), the helical pitch H and the P/D-ratio were varied. The measurements were conducted in air and sodium flow. The results of the studies on helical spacers are plotted in Fig. 9 for $1o^4 < Re < 7 \cdot 1o^4$.

3.2 Local Flow Studies

Local studies of the flow distribution in rod subassemblies were performed to back up the models both in the subchannel computer programs (19-rod subassembly) and in the detailed codes (4-rod subassembly).

A rod subassembly with four parallel rods in a rectangular channel was used to measure

- the distribution of the time-mean velocity
- the distribution of turbulence intensities in the three directions and, hence, the distribution of the kinetic energy of the turbulence
- the distribution of turbulent shear stresses in the directions normal and parallel to the walls and
- the distribution of wall shear stresses.

The measurements were performed by Pitot and Preston tubes and hot wires. The main purpose of these studies is the assessment of the transport properties of turbulent flows in subchannels of rod subassemblies, especially the anisotropy of the exchange of momentum. The results are used to verify and, if necessary, improve the models in existing computer programs and for model development in new computer programs.

The measurements were performed in wall and corner channels of rod subassemblies using different P/D and W/D ratios (see table 1).

Type	P/D	W/D	D(mm)	L/D_h	$Re \cdot 1o^{-4}$	Ref.
wall	1.o71	1.o72	157.5	133	8.73	29,3o,31
wall	1.148	1.148	139.o	97	12.3	32, 31
wall	1.4o2	1.4o1	1oo.o	6o	19.4	33, 31
corner	-	1.o72	157.5	163	5.97	34, 31

Table 1: Main parameters of the studies of the 4-rod subassembly.

The results obtained were measured in great detail, because they were determined at approx. 5oo points in the respective subchannel. The velocity distributions measured by Pitot tubes are represented as contour lines in Fig. 1o for the wall channels with the lowest (1.o7) and highest (1.4) P/D ratio.

All values are referred to a reference velocity of $u_{REF} = 27.7\ ms^{-1}$. Of course, the velocity distribution for P/D = 1.4 is much more uniform. The velocity distributions show no influence of secondary flows. Also the distributions of the kinetic energy of turbulence only exhibit a weak influence of secondary flows in the wall channels, whereas a marked influence of secondary flows in the corner channels can be recognized (Fig. 11), because this channel contains a true corner. The measured values of the kinetic energy of turbulence are referred to the square of a reference wall shear stress velocity.

From the measured velocity distributions and the measured turbulent shear stresses normal and parallel to the walls the eddy viscosities were calculated. In a dimensionless format they can be written down as

$$\varepsilon_r^+ = \frac{-\overline{u'v'}}{L \cdot u^* \, \partial u/\partial r}$$ normal to the wall and (19)

$$\varepsilon_\varphi^+ = \frac{-\overline{u'w'}}{L \cdot u^* \, \partial u/\partial \varphi}$$ parallel to the wall (2o)

In this formula, L is the length of the velocity profile between the wall and the position of maximum velocity and u^* is the local wall shear stress velocity.

The measured eddy viscosities normal to the wall show the same behavior close to the wall as in circular tubes. For $y/L = 0.3$ the measured values are always higher than they are in the circular tube. No dependence on the position on the wall can be found. However, the measured eddy viscosities parallel to the walls exhibit strong dependences both on the position on the wall and normal to the wall (Fig. 12).

The maximum values of the eddy viscosities parallel to the wall are found in the gaps between the rods and between the rod and channel walls, respectively. Anisotropy coefficients ($\varepsilon_{M\varphi} / \varepsilon_{Mr}$) in excess of 200 were measured. With increasing P/D ratio anisotropy decreases.

Comparison of the measured wall shear stress distributions with the results obtained from the VELASCO code for P/D = 1.07 (Fig. 13) shows that the measured wall shear stresses are much more uniform than the calculated ones, although VELASCO contains a model for the secondary flow which also contributes towards establishing more uniform wall shear stress distributions. The main reason of this discrepancy lies in the values of approx. 2 assumed for anisotropy in VELASCO.

A 19-rod subassembly in a hexagonal channel is used to measure the distribution of the time averaged velocities in characteristic subchannel geometries (central, side, corner), /35-38/.

The study serves the following purposes:

- determining the undisturbed, fully developed velocity distribution in the subassembly without spacers to verify computed results from local codes;
- determining the subchannel coolant flows in the subassembly without and with spacers on the basis of the measured velocity fields and investigation of the spacer influenced mass flow separation and redistribution;
- comparison of subchannel mass flow rates determined experimentally with the computed results by global codes.

The measurements are carried out using Pitot tubes. Up to 130 measuring points are recorded per subchannel. The axial coolant distribution is determined by measurements at various distances upstream and downstream of the spacers. The characteristic data of the test section are listed in Table 2.

Number of rods	n = 19
Rod arrangement	hexagonal
Rod diameter /mm/	D = 25
Characteristic ratios /-/	P/D = 1.30
	W/D = 1.17
Axial measuring positions /-/	L_B/D_H = 44; 107
Type of spacer	Spark eroded grid
Hight of spacer /mm/	H_G = 20; 40
Blockage ratios of the spacer	
- central channel /-/	ε_3 = 0.2
- side channel /-/	$\varepsilon_2 \approx$ 0.4; 0.6
- corner channel /-/	$\varepsilon_1 \approx$ 0.4/0.3; 0.6

Table 2: Main data of the test section - Fluiddynamic investigations

The main parameters of the studies conducted so far have been

- Re-number: 3×10^4; 6×10^4
- Spacers: single spacers inserted in pairs
  blockage ratios of the peripheral/central channels

So far, the following most important findings have been derived from the studies /35; 38/.

The undisturbed, fully developed flow distribution was determined as the reference condition. Fig. 14 lists the measured results as an isotach field for a 30° subassembly section for Re = 60,000 and compares them with computed results. The results calculated by means of the VELASCO /5/ and, by ECN, VITESSE codes /11/ showed very satisfactory agreement.

In this way it has been possible to prove that these programs are able to calculate the undisturbed flow distribution for fuel elements with similar geometry conditions. Also the computed mean

subchannel mass flows agree well (< 3%) with the values determined from local measurements. Recalculations by means of the global ARTIS code were less satisfactory initially. Formal improvement by matching to the experimental conditions furnishes results shown in Table 3.

Subchannel type and number (see fig. 16)	1. Experiment		2. VELASCO		3. ARTIS (orig.)		4. ARTIS (modif.)	
	$\dot{m}$ g/sec	%	$\dot{m}$ g/sec	%	$\dot{m}$ g/sec	%	$\dot{m}$ g/sec	%
corner 1	6o	1oo	62	1o3	61	1o3	63	1o5
side 2	79o	1oo	781	99	744	94	784	99
central 3	62o	1oo	624	1o1	643	1o4	625	1o1
central 4+5	63o	1oo	637	1o1	657	1o4	633	1o1

Table 3: Comparison between experimental and calculated mass flow rates /35/.

Velocity fields were measured at various distances (L) downstream of grid type spacers in subassembly geometries now typical. The results proved that there is no undisturbed flow distribution in this case.

This is indicated in Fig. 15 for the subassembly with a spark eroded spacer.

In the isotach field at 3.6 D_h downstream of the spacer the contours of the spacer can still be seen. The following fields indicate the gradual smoothing of the flow. At 18 D_h the local disturbances within the subchannels have balanced out, but undisturbed subassembly flow distribution has not yet been achieved. This is even more evident from Fig. 16.

In this diagram are plotted the axial curves of the mass flows for subchannels 1 to 5 of the subassembly obtained by integration of the measured isotach fields. They are compared with the computed results. It is seen that recalculations of the axial and radial mass flow distributions are hardly satisfactory, both in the original version and in the modified version of the global ARTIS code.

Basic changes of the model included in the computer program are needed now to describe the mass flow redistribution (coolant cross mixing) in the area of the box wall in order to assess the influences of the spacers in the light of the experimental findings obtained.

Variation of the height of the spacers from 2o to 4o mm and variation of the spacer blockages in the subassembly peripheral channels(side and corner) from previously approx. 4o% to 6o% led to the results shown in Fig. 17.

The axial mass flow curves for the side and the adjacent central channel are plotted in this diagram. It shows that the height of the spacers has little influence, whereas the spacer blockages have decisive influences on coolant redistribution. These results constitute important findings with respect to the most suitable design of spacers.

3.3 Local Temperature Studies

A 19-rod subassembly in a hexagonal channel was used in a sodium flow to measure the local temperature distributions in the rod claddings/36; 37; 39-42/

- around the circumferences of the rods in the wrapper tube area
- in the thermal inlet region of the subassembly
- in the area of the grid type spacers, especially underneath the supporting points
- in the case of rod bowing, at the heated end of the subassembly.

The aim of this study is to obtain results to be used for verification, and if necessary, improvement of existing global computer programs and to make them available for the local computer programs now under development.

These are the main characteristics of the test facility:
- up to 19 fuel rod simulators which can be electrically heated indirectly ,
- three adjacent rods, which can be continuously turned by 36o°, in the box wall area with four measuring planes axially displaced by 27 D_h,
- four spark eroded spacers which can be displaced axially across the measuring planes,
- one system for rod bowing at the end of the heated zone.

The main data of the test section are listed in Table 4.

Number of rods	n = 19
Rod arrangement	hexagonal
Rod diameter /mm/	D = 9.o
Characteristic ratios /-/	P/D = 1.3o
	W/D = 1.19
Axial measuring positions /-/	L_B/D_h = 16;43;7o;97
	L_B = O: start of heated length
Type of spacer	Spark eroded grid
Hight of spacer /mm/	H_G = 15
Blockage ratios of the spacer	
- central channel /-/	$\varepsilon_3 \approx$ o.2
- side channel /-/	$\varepsilon_2 \approx$ o.26
- corner channel /-/	$\varepsilon_1 \approx$ o.33/o.5o

Table 4: Main data of the test section - thermodynamic investigation

The experiments performed so far were conducted in the region of 2o < Pe < 1ooo at mean sodium temperatures up to 5oo°C and rod powers up to 37o W/cm, which means that they are in the region of LMFBR operating conditions.

The measured wall temperature distributions in the cladding tubes of a wall rod are shown in Fig. 18 for the four measuring planes /4c

The temperature variations increase continuously with the heated length (L_B/D_h). Because of the highly cooled side channels in this experiment the minimum temperatures are found in the area of the wrapper tube and the relatively broad tempeature peaks on the side of the rod facing the center of the subassembly.

These temperature distributions are influenced by the existing grid type spacers /41/ and by potential rod bowing. Fig. 19 shows the local temperature increase in the cladding wall if one supporting point of the spacer is moved over a temperature measuring point. Upstream and downstream of the grid the temperature gradients are approximately identical. The measuring point outside the support points shows comparatively little temperature changes.

More recent measurements /42/ indicate the influence of pronounced rod bowing at the end of a fuel subassembly upon the local temperature distributions in a adjacent rod claddings. This rod bowing is more pronounced than would be the case merely as a result of tolerances within the subassembly. As an example, Fig. 2o shows the azimuthal temperature distributions of the side rod and of an adjacent central rod for three different bowing positions.

This shows that the continuous cross section reduction of a subchannel brought about by rod bowing results in clear temperature increases only locally, i.e., in the areas of the cladding tubes directly bordering upon the subchannel involved. In rods of the next row, no major temperature changes are found for this case.

These experimental results furnish detailed data verifying local computer programs under development and global computer programs used for the design of LMFBR fuel elements.

While recalculations of experimental results generated in fluid dynamic tests have produced their first positive results, detailed calculation of the local temperature distributions in the fuel element components is not yet possible. This finding is explained in an example in Fig. 21.

In addition to the measured azimuthal temperature distribution of the side rod the mean values of the subchannel temperatures computed by means of ARTIS and the mean temperatures of cladding tube sectors calculated on this basis by various heat transfer relations are plotted. The maximum azimuthal differential temperatures compared here, which stem for calculations and experiments, result in computed values which are lower by a factor of 2...6. This clearly results in the need to improve global codes and to develop local codes and adapt them to suitable experiments so as to permit more precise calculations to be performed in the critical zones (wrapper tube region) of fuel elements /36/.

4. Conclusions for Future Work

In the light of the experience obtained in current design calculations and experimental studies and also in the light of experiences accumulated in the core element behavior of reactors now in operation, a number of further studies are thought to be urgently required in view of future code developments.

For improvement of the subchannel computer programs it is necessary to

- determine with more precision the distribution of the fuel rod cladding temperature, especially in the edge zones of the fuel elements, also in nominal geometries,
- calculate with a higher degree of reliability the mass flow redistributions in the area of grid type spacers.

  for this purpose, knowledge of the drag coefficients in the subchannels is decisive,
- make amenable to calculation temperature distribution in disturbed geometries by effects depending on burnup, such as swelling and bowing of structures,
- include the calculations flow conditions in mixed convection.

To achieve these goals, more experimental studies are needed. However, global experimental studies can achieve progress with respect to these goals only through a large number of expensive experiments with sufficient statistical data, because the number of parameters to be fitted and empirical relations to be introduced into the models is large and also because the individual effects cannot be separated from global studies. For this reason, it is proposed to perform more detailed analyses than would be possible in subchannel computer programs for such important subareas as

- temperature distribution in the side/corner channels
- effects of flow development
- non-nominal geometries
- effects of spacer grids on flow and temperature distributions.

The empirical dependencies to be introduced into the subchannel computer programs can then be obtained by parameter studies by means of detailed codes. For this reason speedy further development of detailed codes is necessary which must also be backed experimentally. Experimental studies on the verification of detailed codes can be performed in simpler geometries on an enlarged scale at reasonable expenditure. This includes studies of the velocity distribution, distributions of the kinetic energy of turbulence, eddy viscosities and secondary flows and wall shear stresses in characteristic subchannels of rod subassemblies, i.e.,

- without spacers for fully developed and developing flows
- in the spacer region and in the flow area affected by the spacer grids and
- for non-nominal geometries and flow situations.

To calculate detailed temperature distributions in the fuel rod and fluid regions it is also necessary to determine experimentally in sodium the turbulent thermal conductivities and turbulent Prandtl numbers, respectively, and their anisotropy and dependence on geometry, in characteristic subchannels of rod subassemblies

- without spacers for fully developed and developing flows
- in the region of the flow zone affected by spacers and
- for non-nominal geometries and flow situations.

For verification of the code developments a final experimental study in sodium in a rod subassembly with ≥ 19 rods with grid type spacers and the possibility to simulate bows and geometry

deformations would be very important. In such experiments, the instrumentation should allow detailed measurements to be performed of the temperature and velocity distributions at various levels (inlet).

Nomenclature

C_{sk}	/-/	constant
c	/-/	constant
D	/m/	rod diameter
D_h	/m/	hydraulic diameter
EF	/-/	intensity parameter (empirical)
F	/m^2/	flow cross section
F_k	/m^2/	free channel cross section of wall or corner channels
H	/m/	helical lead
h	/J/	enthalpy
i	/-/	number of spacer grids
k	/$Wm^{-1}k^{-1}$/	thermal conductivity
L	/m/	length
l	/m/	mixing length
$\dot{m}$	/kgs^{-1}/	mass flow rate
P	/m/	pitch of the rods
Pe	/-/	Peclet number
Δp	/Nm^{-2}/	pressure drop
q	/Wm^{-2}/	heat flux
Re	/-/	Reynolds number
r	/m/	co-ordinate normal to the wall
S_e	/m/	perimeter
s	/m/	gap between rod and shround
u	/ms^{-1}/	velocity
u^+	/-/	non-dimensional velocity
u'	/ms^{-1}/	fluctuating velocity in axial direction
u^*	/ms^{-1}/	friction velocity
v	/ms^{-1}/	periphered secondary velocity
v'	/ms^{-1}/	fluctuating velocity in direction normal to the wall
W	/m/	gap between rod and wrapper tube and rod diameter
w'	/ms^{-1}/	fluctuating velocity parallel to the wall
y	/m/	distance from the wall
y^+	/-/	non-dimensional distance from the wall
z	/m/	co-ordinate in axial direction
ε	/-/	blockage ratio of spacer grids
ε_q	/m^2s^{-1}/	eddy conductivity
ε_M	/m^2s^{-1}/	eddy viscosity
κ	/-/	constant
λ	/-/	friction factor
μ	/m^{-1}/	mixing factor
ϱ	/kgm^{-3}/	density
ψ	/-/	inverse turbulent Prandtl number
φ	/deg/	coordinate parallel to the wall
τ	/Nm^{-2}/	shear stress
ζ	/-/	grid drag coefficient

Indices

r	normal to the wall
φ	parallel to the wall
w	at the wall
o	smooth tube

References:

/ 1/ W. Baumann
MISTRAL-II, Thermohydraulische Mischströmungsalgorithmen für Stabbündel.
KfK 1605, Juni 1972

/ 2/ G. Straub
Berechnung der Temperatur- und Geschwindigkeitsfelder in parallel angeströmten Brennstabbündeln schneller natriumgekühlter Brutreaktoren.
Dissertation, IKE, TU Stuttgart 1976

/ 3/ K. Doetschmann, A. Amendola
THECA - Ein Programmsystem zur dreidimensionalen thermo-hydraulischen Auslegung, schneller Reaktorkerne.
KfK 2372, März 1977

/ 4/ H. Hoffmann
Experimentelle Untersuchung zur Kühlmittelquervermischung u. zum Druckabfall in Stabbündeln mit wendelförmigen Abstandshaltern.
KfK 1843, Dez. 1973

/ 5/ W. Eifler, R. Nijsing
VELASCØ - Velocity Field in Asymmetric Rod Configurations.
EUR-4950e (1973)

/ 6/ Z. Farago
interner Bericht (1978)

/ 7/ L. Prandtl
Über die ausgebildete Turbulenz
ZAMM 5 (1925) 146

/ 8/ R. van Driest
On turbulent flow near a wall
J. Aerosp. Sci. 23(11) (1956)

/ 9/ J. Nikuradse:
Gesetzmäßigkeit der turbulenten Strömung in glatten Rohren.
V.D.I. Forsch. 281, 1926

/10/ R. Meyder
Bestimmung des turbulenten Geschwindigkeits- und Temperaturfeldes in Stabbündeln mit Hilfe von krummlinig-orthogonalen Koordinaten.
KfK 2029 (1974)

/11/ W. Slagter, H.A. Roodbergen, N.H.Decker:
Prediction of Fully Developed Turbulent Flow in Non Circular Channels by the Finite Element Method, NATO Advanced Study Institute,Istanbul, (1978)

/12/ G. Grötzbach
Direkte numerische Simulation turbulenter Geschwindigkeits- Druck- u. Temperaturfelder bei Kanalströmungen
KfK 2426, Okt. 1977

/13/ G. Grötzbach
Num. Untersuchungen der Quervermischung bei auftriebsbeeinflußter turbulenter Konvektion in einen vertikalen Kanal
KfK 2648, Juni 1978

/14/ H. Hoffmann
Ergebnisse der Vergleichsrechnungen von Temperaturfeldern bei Natriumkühlung, in: Thermo- und fluiddynamische Unterkanalanalyse der Schnellbrüter-Brennelemente und ihre Relation zur Brennstabmechanik.
KfK 2232 (1975), p. 39-108

/15/ H. Hoffmann
Unterkanalanalyse und Brennelementauslegung, Zusatzaufgaben in den Vergleichsrechnungen,
unveröffentlicht (1977)

/16/ K. Rehme
Pressure drop performance of rod bundles in hexagonal arrangements.
Int. J. Heat Mass Transfer 15, 2499-2517 (1972)

/17/ J. Marek, K. Maubach und K. Rehme
Heat transfer and pressure drop performance of rod bundles arranged in square arrays.
Int. J. Heat Mass Transfer 16, 2215-2228 (1973)

/18/ K. Rehme
Laminar flow through rod bundles,
Chemie-Ing.-Technik 43, 962-966 (1972)(in German)

/19/ K. Rehme
Simple method of predicting friction factors of turbulent flow in non-circular channels.
Int. J. Heat Mass Transfer 16, 933-950 (1973)

/20/ K. Rehme
Drag coefficients of spacer grids in fuel elements.
ATKE 15, 127-130 (1970) (in German)

/21/ K. Rehme
Pressure drop correlation for fuel element spacers.
Nucl. Technology 17, 15-23 (1973)

/22/ K. Rehme
Pressure drop of spacer grids in smooth and roughened rod bundles.
Nucl. Technology 33, 314-317 (1977)

/23/ K. Rehme
The pressure drop of spacer grids in rod bundles of 12 rods with smooth and roughened surfaces.
Report KfK 2697 (1978)

/24/ K. Rehme
Systematische experimentelle Untersuchung der Abhängigkeit des Druckverlustes von der geometrischen Anordnung für längsdurchströmte Stabbündel mit Spiraldrahtabstandshaltern.
Dissertation, TU Karlsruhe (1967)

/25/ P.E. Huber
Experimentelle Untersuchungen des Druckabfalles in eng gepackten Stabbündeln mit wendelförmigen Abstandshaltern.
Studienarbeit (1978) (unveröffentlicht)

/26/ W. Baumann, R. Möller
Experimental Study of coolant cross-mixing in multirod-bundles.
Atomkernenergie 14-56 (1969)

/27/ H. Hoffmann, E. Baumgärtner, H.H. Frey
Experimentelle Untersuchungen zur Kühlmittelquervermischung an Stabbündeln mit gitterförmigen Abstandshaltern bei turbulenter Natrium-Strömung.
KfK 2360 (1977)

/28/ E. Baumgärtner, H. Hoffmann
Untersuchungen zur Kühlmittelquervermischung in natriumgekühlten Brennelementen.
KfK 1275/2 (1975), p. 126/8 -10

/29/ K. Rehme
Experimental investigation of the turbulent flow through a wall subchannel of a rod bundle.
Report KfK 2441 (1977) (in German)

/37/ H. Hoffmann, R. Möller, H. Tschöke, G. Trippe, D. Weinberg
Thermo- und fluiddynamische Untersuchungen an Brennstabbündeln.
KfK-Nachrichten, Vol. 10, 3/4 (1978), p. 32-36

/38/ G. Trippe
Experimentelle Untersuchung der Strömung in axial durchströmten Stabbündeln hexagonaler Anordnung bei großen Re-Zahlen und unter Berücksichtigung der Wirkung von gitterförmigen Abstandshaltern.
(1979) - unveröffentlicht

/39/ R. Möller, H. Tschöke, M. Kolodziej
Experimentelle Bestimmung von Temperaturfeldern in Natriumdurchströmten Bündeln mit hexagonaler Stabanordnung und gitterförmigen Abstandshaltern.
KfK 2356 (1977)

/40/ R. Möller, H. Tschöke
Experimental Determination of Wall Temperature Fields in Rod Bundle Geometries with Turbulent Sodium Flow.
6th International Heat Transfer Conf.;Vol 5, p. 29-34, Toronto 1978

/41/ R. Möller, H. Tschöke
Experimentelle Bestimmung der lokalen Temperaturfeldänderung in den Hüllrohren eines natriumdurchströmten Stabbündels durch gitterförmige Abstandshalter.
DatF/KTG-Reaktortagung, Hannover, 1978, p. 110-113

/42/ R. Möller, H. Tschöke
Influence of Rod Bowing on the Measured Local Temperature Distribution in Fuel Rod Cladding Tubes with Sodium Cooling.
European Nuclear Conf., Hamburg 1979

/30/ K. Rehme
The structure of turbulent flow through a wall subchannel of a rod bundle.
Nucl. Engng. Design 45, 311-323 (1978)

/31/ K. Rehme
Non-isotropic eddy viscosities in turbulent flow through rod bundles.
NATO Advances Study Institute, Istanbul (1978)

/32/ K. Rehme
Turbulent flow through a wall subchannel of a rod bundle.
Report KfK 2617 (1978) (in German)

/33/ K. Rehme
Velocity and turbulence distributions in a wall subchannel of a rod bundle.
Report KfK 2637 (1978) (in German)

/34/ K. Rehme
Measurements of the velocity-, turbulence-, and wall shear stress distributions in a corner subchannel of a rod bundle.
Report KfK 2512 (1977) (in German)

/35/ G. Trippe, D. Weinberg
Experimental and Theoretical Investigations of Turbulent Velocity Distribution in Rod Bundles With and Without Grid-Type Spacers.
NATO Advanced Study Institute, Istanbul (1978)

/36/ R. Möller, D. Weinberg, G. Trippe, H. Tschöke
Experiments on the Fluiddynamics and Thermodynamics of Rod Bundles to Verify and Support the Design of SNR-300 Fuel Elements. - Status and Open Problems.
IAEA-SM-225/34, Bologna 1978

CODE	APPLICATION	DESCRIPTION	PARTICULARITIES
MISTRAL-II	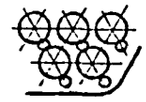	Rod Bundle 3-dim.bulk-temp.	with spacers
ARTIS	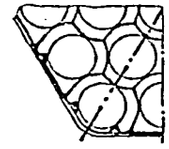	Rod Bundle 3-dim.bulk-velocity and bulk temp.	with grid spacers
THECA	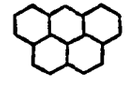	Core 3-dim. bulk and wrapper tube temp. hot spot anal.	with spacers
VELASCO	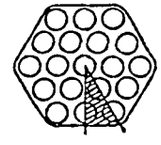	Rod Bundle/ Segment (infinite and finite rod arrays) 3-dim.turbulent momentum and energy transport	without spacer
VERA TERA	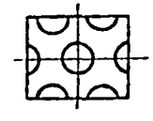	Rod Bundle Segment general curvilinear orthogonal coordinates 3-dim.turb.momentum and energy transp.	without spacer
TURBIT-3	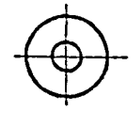	Annulus 3-dim. transient turbulence transp. loc.velocities and temp.	without spacer

FIG. 1: THERMO AND FLUID DYNAMIC CODES

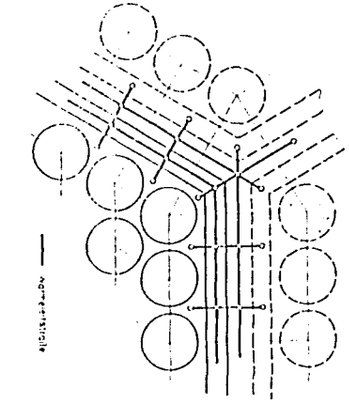

Fig.2: Heat transfer through the wrapper tube

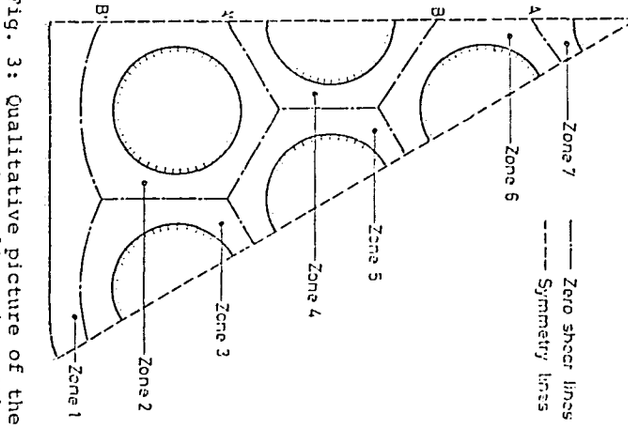

Fig. 3: Qualitative picture of the zero shear lines in a subarray representative for a thirty-seven rod array

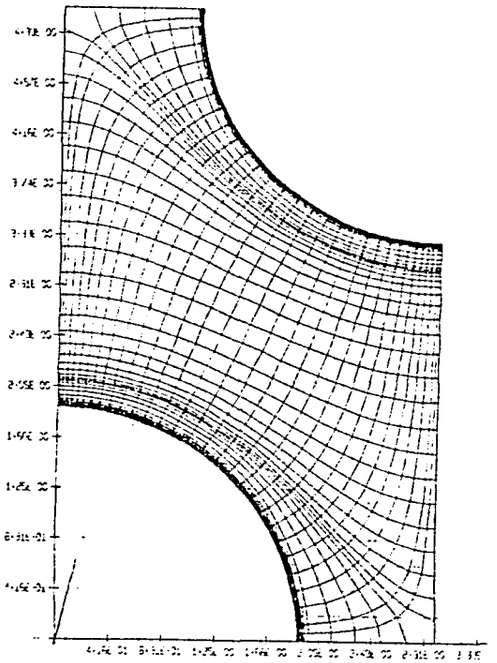

Fig. 4: Curvilinear-orthogonal coordinates

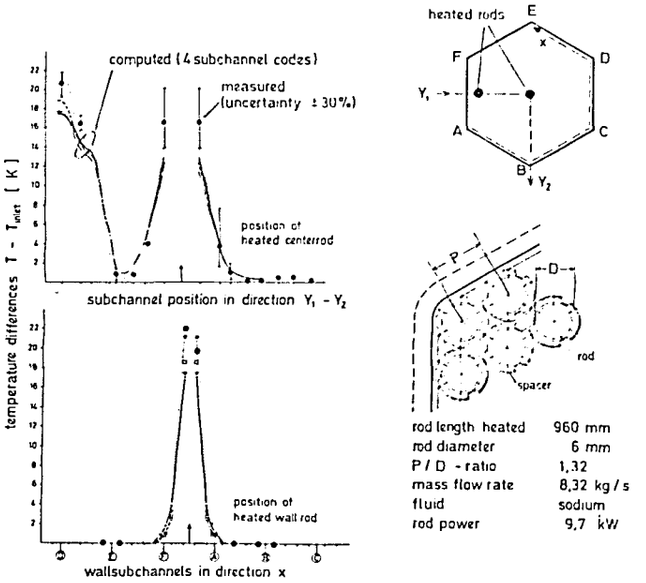

Fig. 5: Mean subchannel temperatures: Comparison between computed and experimental results /14/

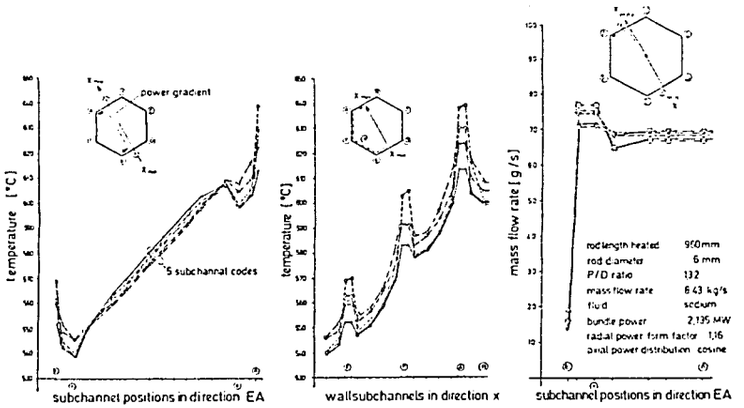

Fig. 6: Mean subchannel temperatures and mass flow rates
Comparison between computed results /15/

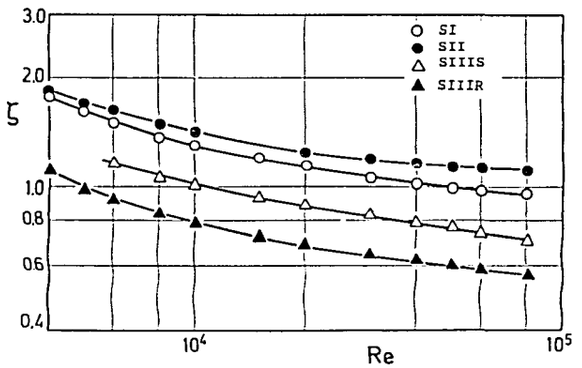

Fig. 7: Drag coefficients of various grid type spacers

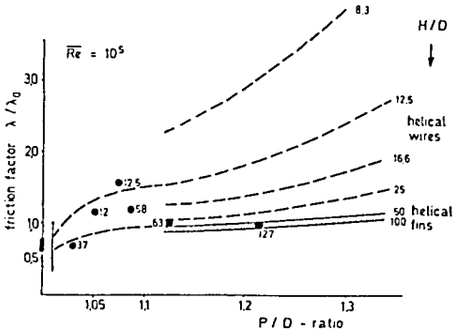

Fig. 8: Friction factors as function of P/D and H/D-ratio for 61 rod bundles wire helical spacer types (37/61-rod bundles)

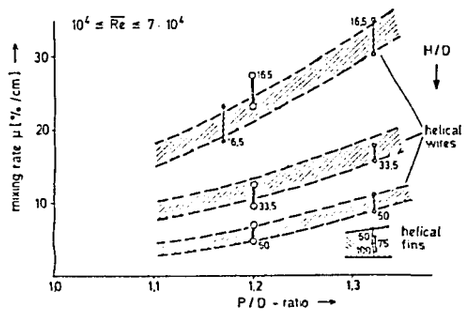

Fig. 9: Mixing coefficients as function of P/D and H/D-ratio for 61-rod bundles with helical spacer types

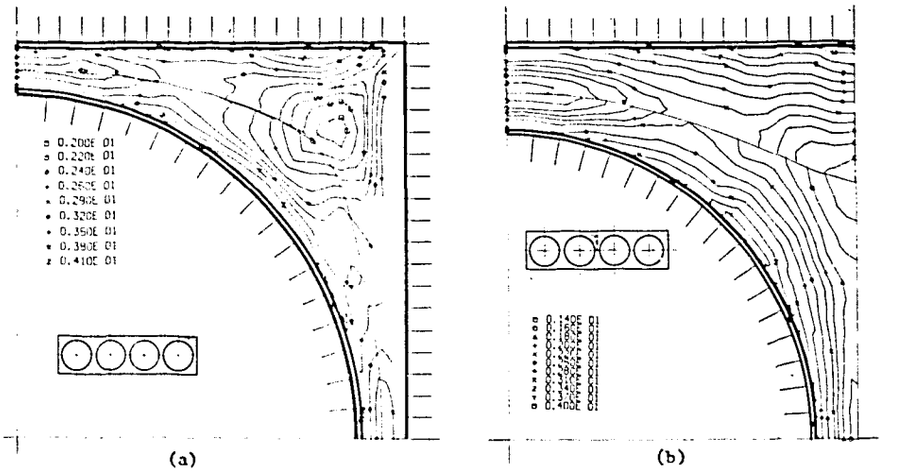

Fig. 11: Kinetic energy of turbulence $\overline{k'}/u^{*2}_{REF}$
(a) in a corner subchannel W/D = 1.07; (b) in a wall subchannel P/D = 1.15

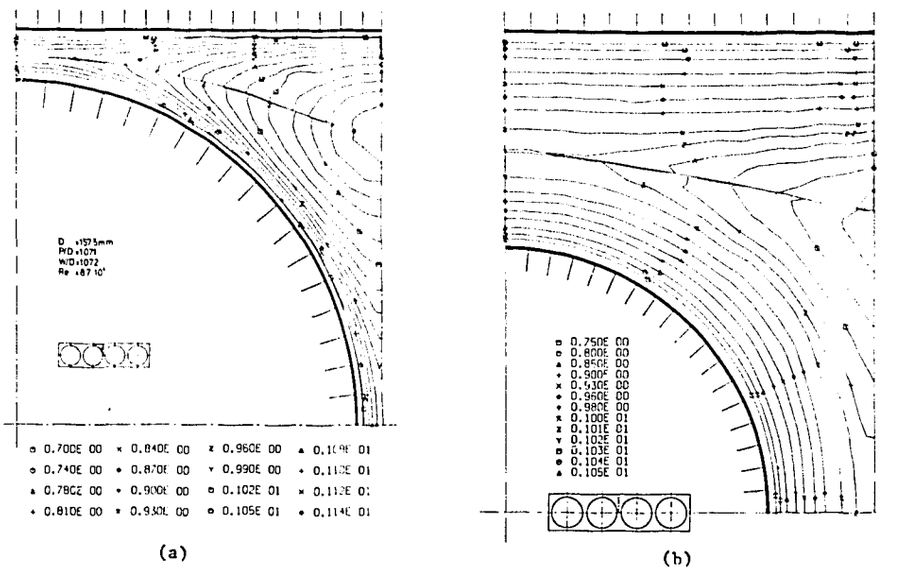

Fig.10: Velocity distributions u/u_{REF} measured in wall subchannels (a)
(a) P/D = 1.07; (b) P/D = 1.4

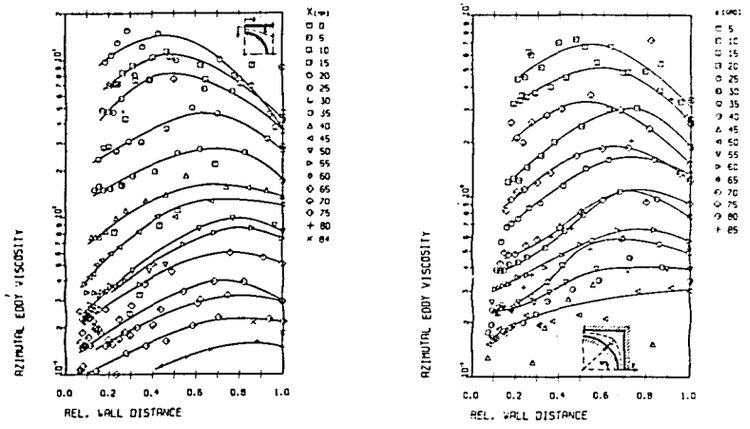

Fig. 12: Dimensionless eddy viscosity parallel to the channel wall in the wall channel (P/D = 1.07) and corner channel (W/D = 1.07) as a function of the dimensionless distance from the wall

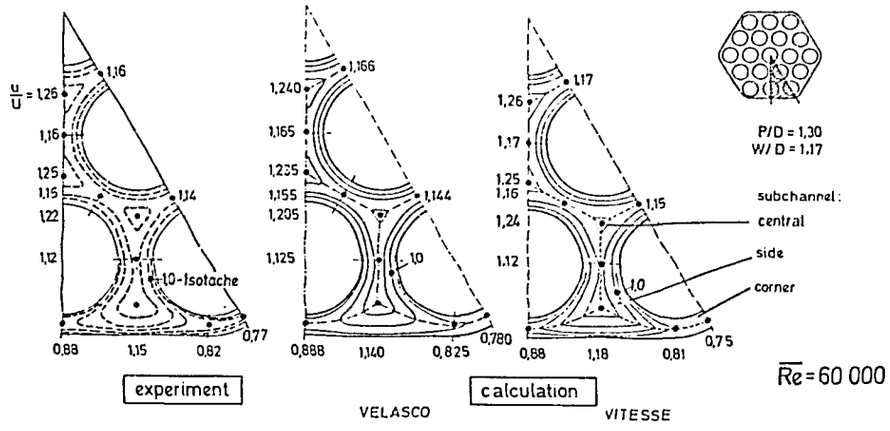

Fig. 14: Fully developed velocity distribution in 19 rod bundle (Re = 60 000; P/D = 1.30; W/D = 1.17)

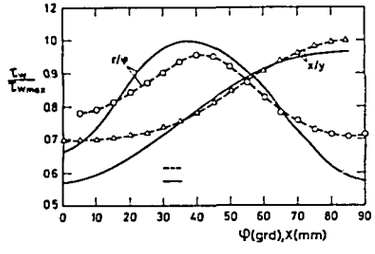

Fig. 13: Comparison of the measured wall shear stress distributions in the wall channel (P/D = 1.07) with VELASCO-results

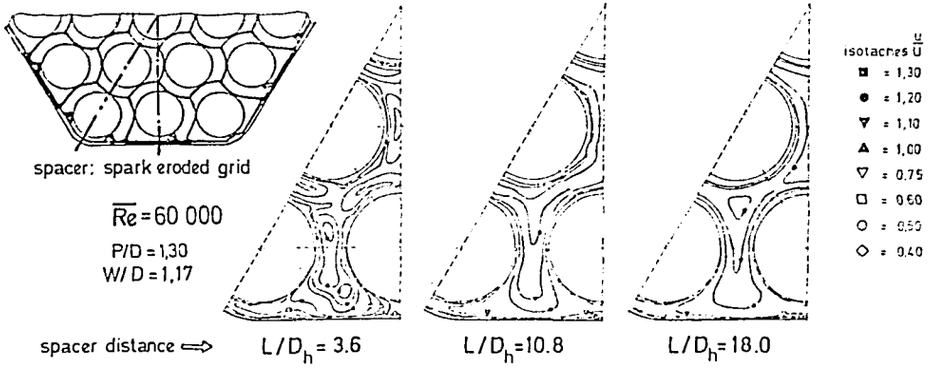

Fig. 15: Axially developing velocity profiles in 19-rod bundle behind grid spacer (Re = 60 000; P/D = 1.30; W/D = 1.17)

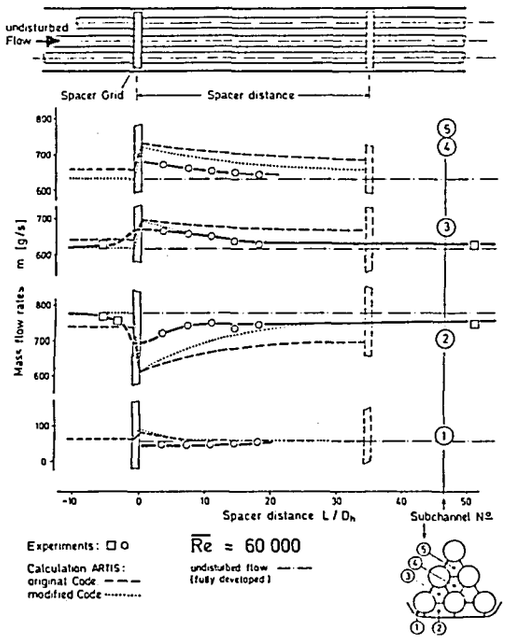

Fig. 16: Mass flow distribution in 19 rod-bundle with grid spacer (Re = 6o ooo; P/D = 1.3o;W/D = 1.17)

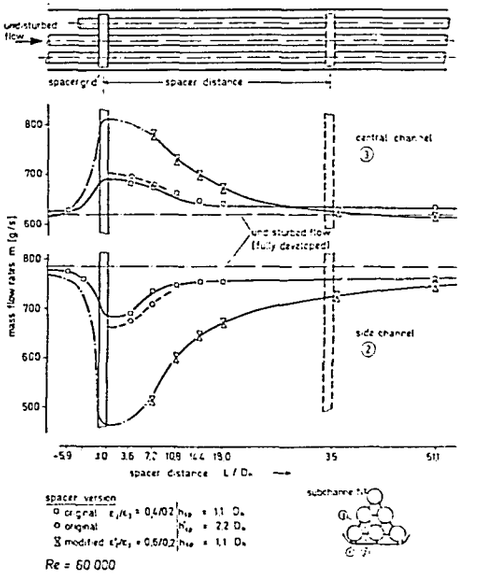

Fig.17: Mass flow distribution in 19-rod bundle with varying grid spacer blockages and grid heights (Re = 6o ooo; P/D = 1.3; W/D = 1.17)

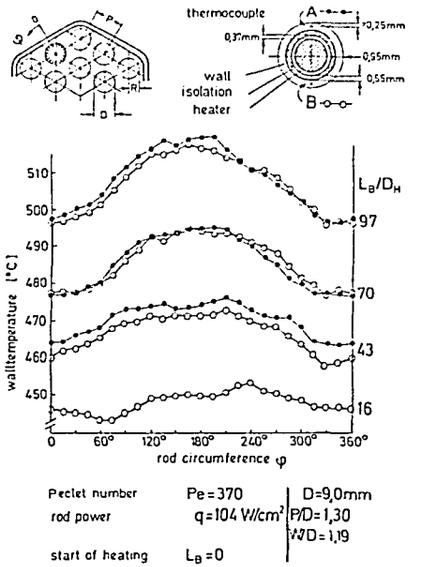

Fig. 18: Temperature distribution in 19-rod bundle at the circumference of the side rod (Pe = 17o; P/D = 1.3; W/D = 1.19; q = 1o4 W/cm^2)

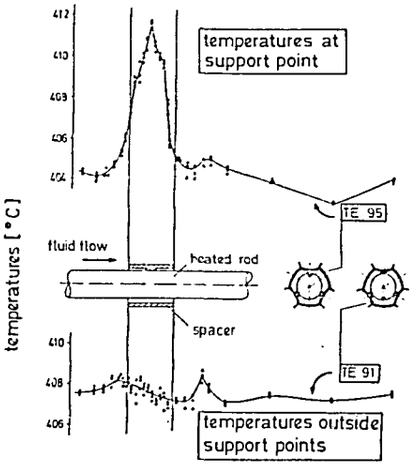

Fig. 19: Axial temperature distribution of a rod in the spacer region (Pe = 346; P/D = 1.3; W/D = 1.19: q = 73 W/cm^2; L_B/D_h = 97)

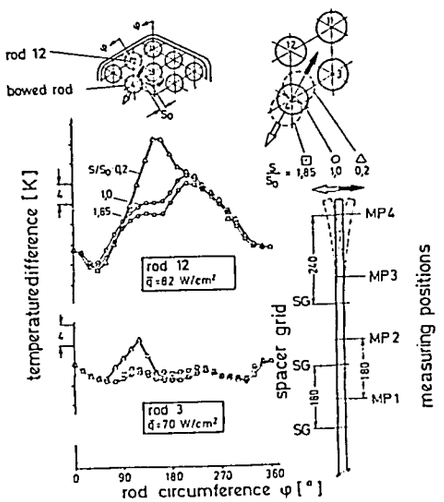

Fig. 20: Cladding temperatures for different bowing positions (Pe = 370; P/D = 1.3; W/D = 1.19; L_H/D_H = 97)

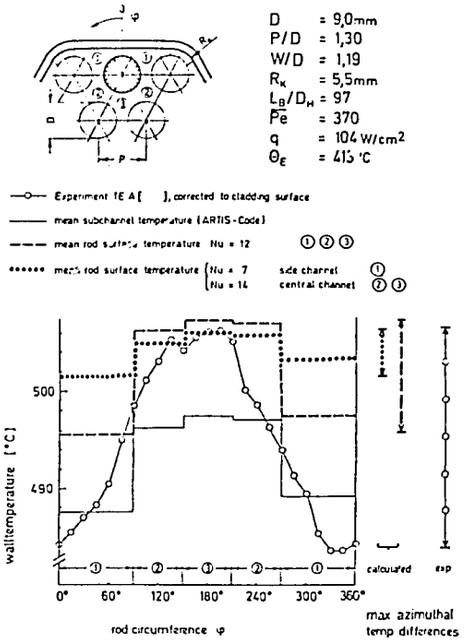

Fig. 21: Azimuthal temperature variation of the side rod cladding: Comparison between local measurements - global calculations